Supplemental Information

Supplemental Figure 1. Postnatal development of Glis3KO mice is accompanied by growth retardation. Total body weights of WT and Glis3KO mice were measured at the indicated times. Data were shown as mean ± SEM (n ≥8 for each group). Student's t test. * $p<0.05$, ** $p<0.001$.

Supplemental Figure 2. Apoptotic cells were not observed in thyroid glands from WT and Glis3KO mice. Thyroids from 1 month old WT and Glis3KO mice were examined for the presence of apoptotic cells by TUNEL assay using an *In Situ* Cell Death Detection Fluorescein Kit and DAPI as described in Materials and Methods. Scale bar: 50 μm.

Supplemental Figure 3. Analysis of blood T4 levels in one week old WT and Glis3KO mice. Although there was a tendency to lower circulating T4 levels in Glis3KO mice, the difference was not statistically significant. Data were shown as mean ± SEM (n ≥6 for each group). Student's t test.

Supplemental Figure 4. Volcano plot of RNA-Seq gene expression profiles of WT and Glis3KO thyroid glands. RNA isolated from thyroid glands of WT-LID and KO-LID mice were analyzed by RNA-Seq. Global pattern of expression was shown as a volcano plot with fold change (Log_2) and *P* value ($-log_{10}$). Genes with $\geq$2 fold change and a *P* value $\leq$0.05 are indicated by red dots. Specific genes are indicated by green triangles.

Supplemental Figure 5. Proliferation of thyroid follicular cells was greatly reduced in KO mice. (**A**) The number of phosphorylated histone H3 (pH3) positive cells (Green) was examined in thyroid glands of WT and Glis3KO mice fed either a ND or LID by immunofluorescent staining. Wheat germ agglutinin (WGA, Red) was used to define thyroid epithelial cells. Scale bar: 50 μm. (**B**) The number of $pH3^+$ cells was counted and plotted (n ≥2 for each group). Student's t test. * $p<0.05$, ** $p<0.001$.

Supplemental Figure 6. Levels of phosphorylated AMPK and PKA were not altered in thyroid glands of Glis3KO mice. Protein lysates obtained from thyroid glands of WT and Glis3KO mice fed either a ND or LID were examined by Western blot analysis using phospho-AMPK, phosphor-PKA, and GAPDH antibodies.

Supplemental Figure 7. The expression of TTF1 protein was not significantly different between thyroid glands of WT and Glis3KO mice. Representative images of sections of WT and Glis3KO thyroid glands examined by immunohistochemistry with antibodies against TTF1 (red) and PECAM (green). Scale bar: 50 μm.

Supplemental Figure 8. Heatmap of the density of GLIS3-ChIP signals within a 5-kb window surrounding predicted GLIS3 peaks. Each line in the heatmap represents an individual GLIS3 binding site (read count = 15,920). Lower panel: Plot of the average density of GLIS3-ChIP signals relative to GLIS3 peaks.

Supplemental Figure 9. Venn diagram of gene-sets enriched for GLIS3-associated genes, and genes up- or down-regulated in the thyroid glands of KO-LID mice. RNA-Seq analysis identified 3420 differentially expressed genes, while ChIP-Seq analysis identified 3374 GLIS3-associated genes of which 453 genes were differentially expressed.

Supplemental Figure 10. GLIS3 was enriched at the NUE region of the *Nis* gene. (A) ChIP-PCR was performed to validate the enrichment of GLIS3 at the -1kb and -2.8 kb (NUE region) of the *Nis* upstream promoter in thyroid glands from WT and Glis3-EGFP mice. (B) Genome browser shot of the GLIS3-EGFP occupancy at the *Nis* genome as identified by ChIP-Seq analysis. (C) PAX8 occupancy at the *Nis* genome was extracted from a previous report (1) and visualized as a gene browser shot. Both GLIS3 and PAX8 bind the NUE enhancer region in the *Nis* promoter. Data were shown as mean ± SEM (n=3 for each group). Student's t test. * $p<0.05$.

Supplemental Figure 11. Activation of NUE promoter by GLIS3. A luciferase reporter driven by the NUE promoter region (pTAL-NUE) was used to examine the transcription activation by Glis3 and PAX8 in HEK293T cells. Data were shown as mean ± SEM (n=3 for each group). Student's t test. * $p<0.0001$, compared to first lane.

Supplemental Figure 12. GLIS3 did not interact with PAX8 or TTF1. Human kidney HEK293T cells were transfected with p3XFLAG-CMV-HA expressing either full-length

GLIS3, N-terminus deletion mutant GLIS3ΔN, or C-terminal deletion mutant GLIS3ΔC, with or without pcDNA-Ttf1 or pcDNA-Pax8 as indicated. After 24 h incubation, GLIS3-HA protein complexes were isolated with anti-HA antibody and examined by Western blot analysis with antibodies against HA and TTF1 or PAX8. Cotransfection with p3XFLAG-CMV-HA-GLIS3FL and pCMV-Sufu-Myc was used as a positive control. Data shown are representative of two independent experiments.

Supplemental Table 1. Pathway analysis was performed with genes down-regulated in thyroid glands from Glis3KO mice fed a ND using various databases, including KEGG (A), Reactome (B), and Biocarta (C), or genes up-regulated in thyroid glands from Glis3KO mice fed a ND using a KEGG pathway analysis (D). Gene expression data were generated by microarray analysis.

Supplemental Table 2. Pathway analysis was performed with genes down-regulated in thyroid glands from KO-LID mice using various databases, including KEGG (A), Reactome (B), and Biocarta (C), or GO biological process (D). Gene expression data were generated by RNA-Seq analysis.

Supplemental Table 3. Fold-change in the expression of a selected number of genes that are regulated directly or indirectly by GLIS3. The expression and GLIS3 occupancy of a selected number of genes related to cell cycle/proliferation, TH biosynthesis, fibrosis/ECM, and inflammation are compared between thyroid glands from Glis3KO and WT mice fed either a ND or LID. Gene expression data were derived by

microarray or RNA-Seq analysis, and GLIS3 occupancy by ChIP-Seq analysis as indicated. In the column with ChIP-Seq results: +, indicates enrichment for GLIS3 binding within the respective gene; -, no enrichment.

Supplemental Table 4A. List of all GLIS3 target genes identified by ChIP-Seq analysis. Pathway analysis was performed using various databases, including KEGG (B), Reactome (C), and Biocarta (D), and analysis of GO biological process (E).

Supplemental Table 5A. List of genes identified by ChIP-Seq that are down-regulated in thyroid glands of Glis3KO mice fed a LID. B. List of genes identified by ChIP-Seq that are up-regulated in thyroid glands of Glis3KO mice fed a LID. C. GO biological process analysis of genes identified by ChIP-Seq that are down-regulated in thyroid from Glis3KO mice fed an LID using a program from David Bioinformatics Resources.

Supplemental Table 6.

List of primers used for QRT-PCR analysis.

60. Ruiz-Llorente S, et al. Genome-wide analysis of Pax8 binding provides new insights into thyroid functions. BMC Genomics. 2012;13:147.

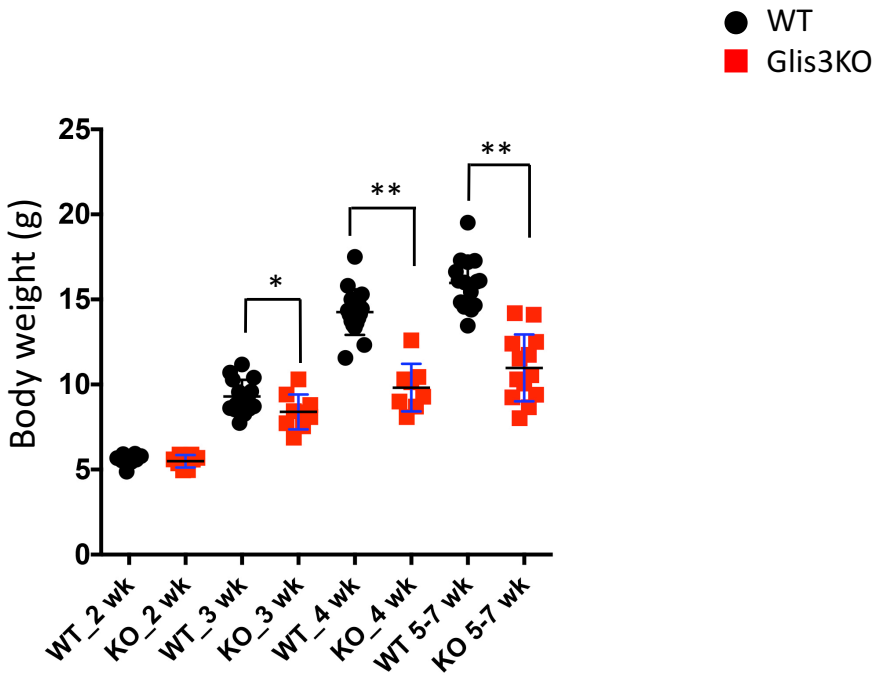

Supplemental Figure 1

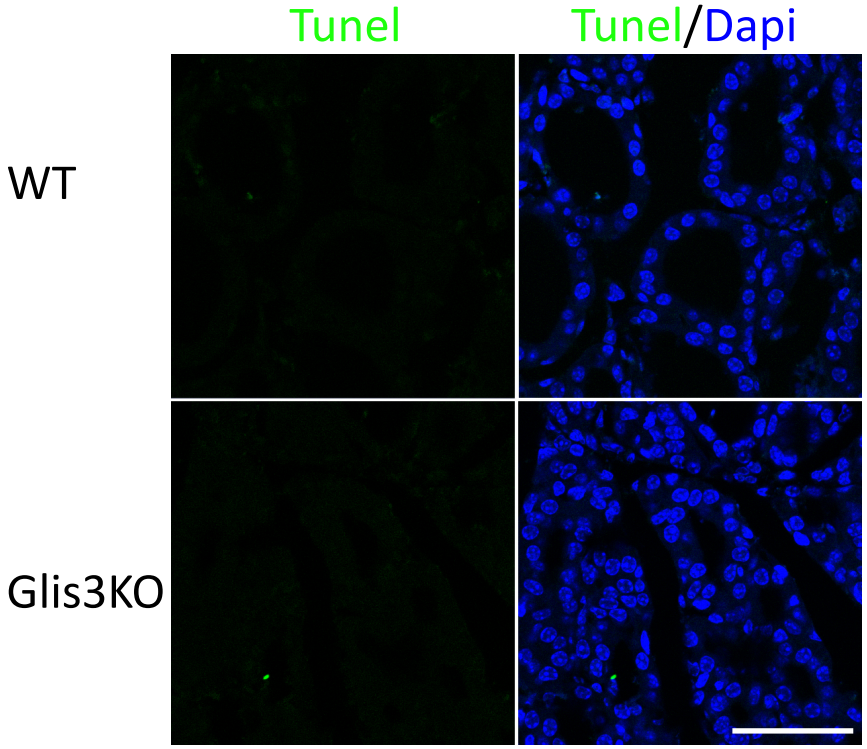

Supplemental Figure 2

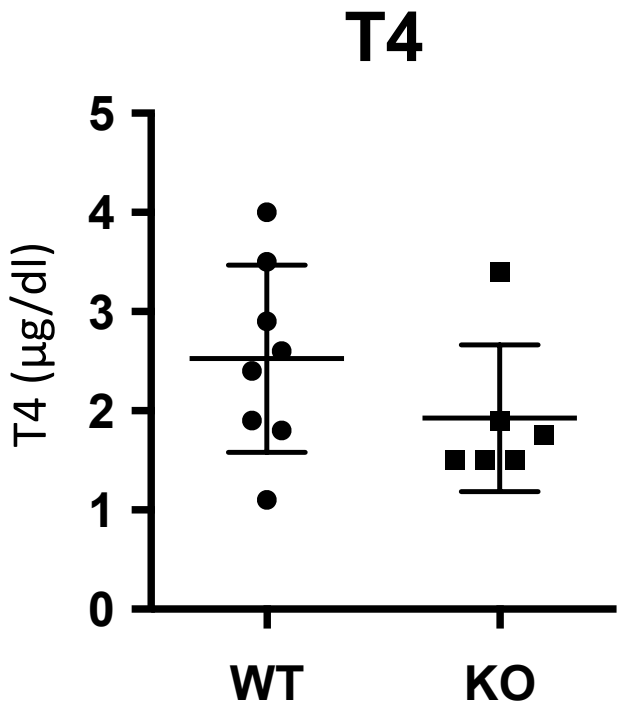

Supplemental Figure 3

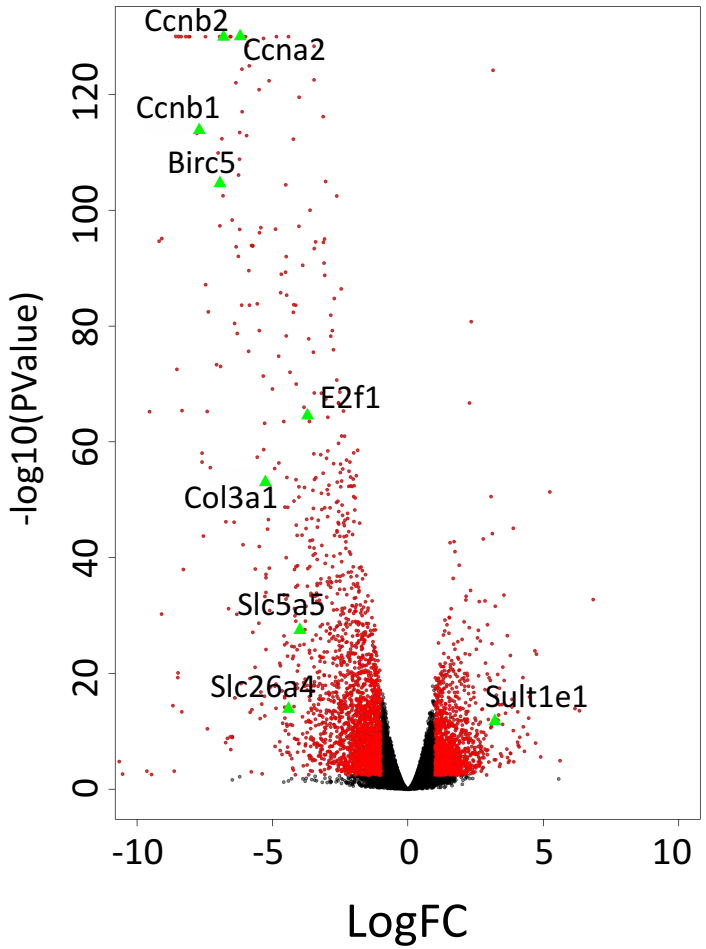

Supplemental Figure 4

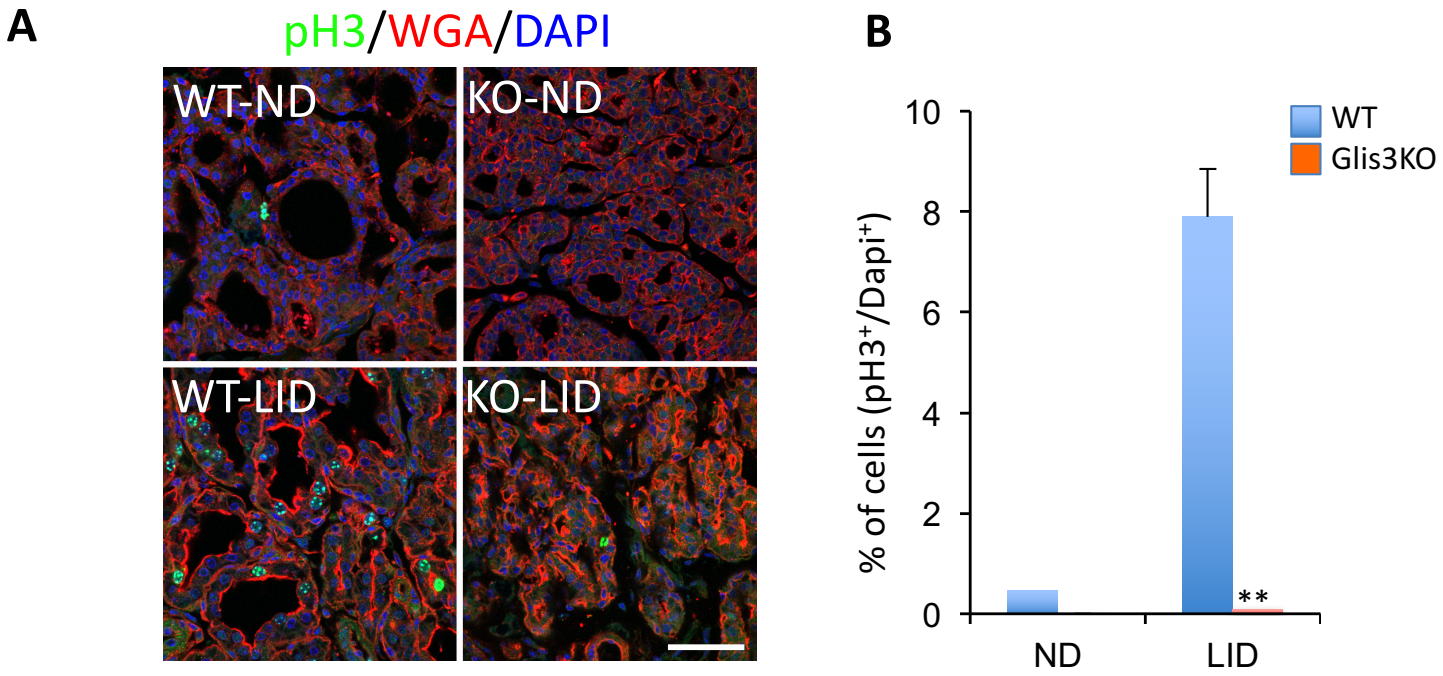

Supplemental Figure 5

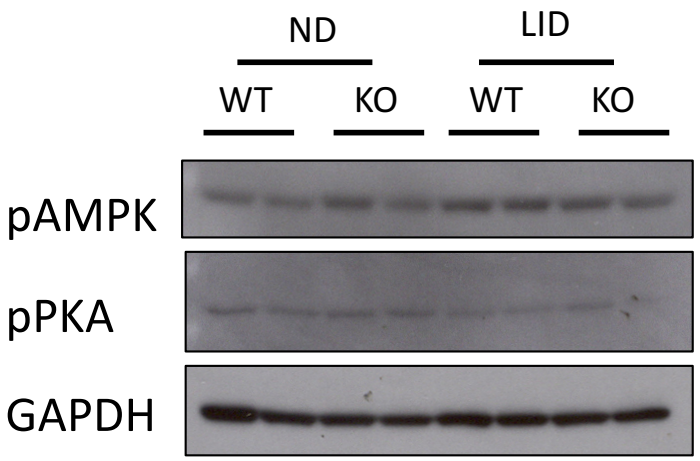

Supplemental Figure 6

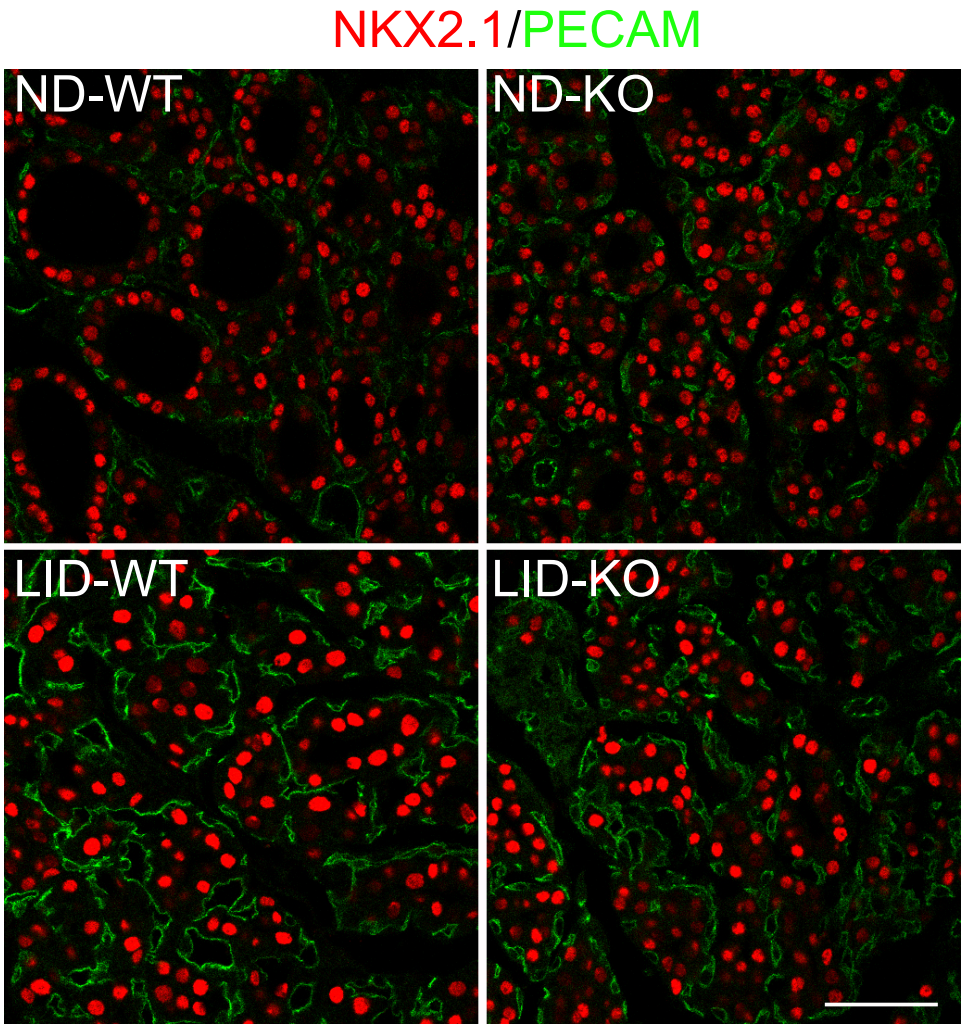

Supplemental Figure 7

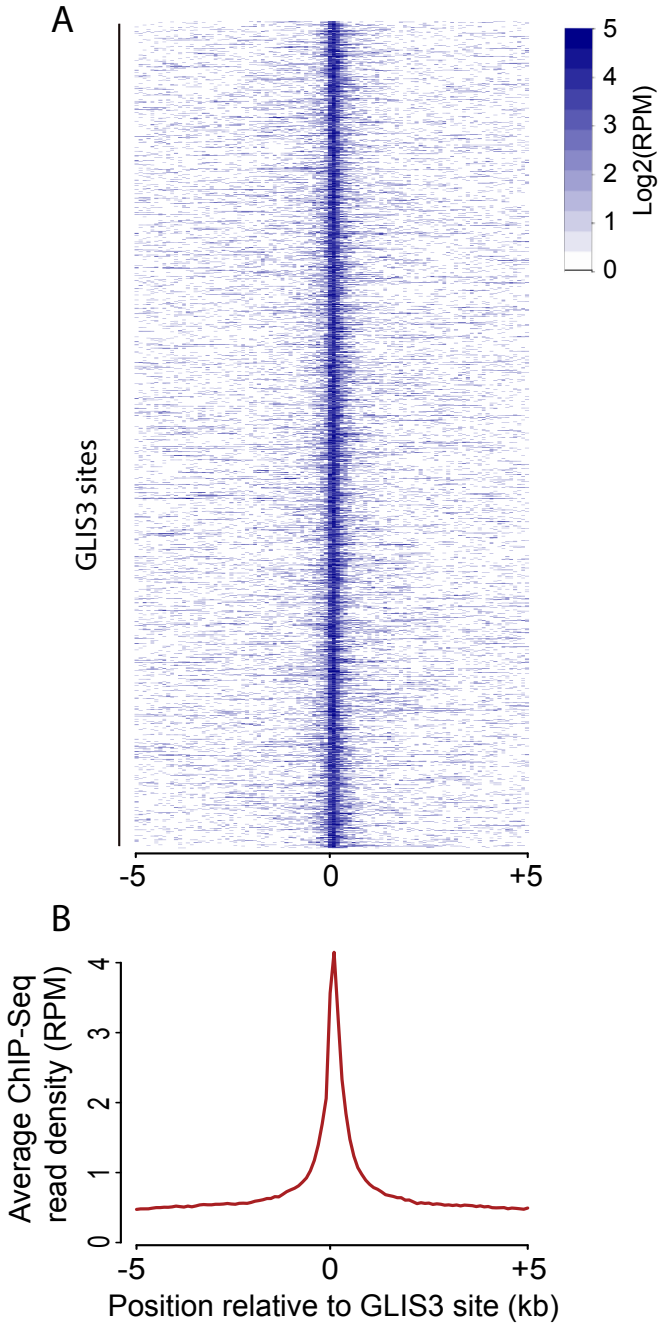

Supplemental Figure 8

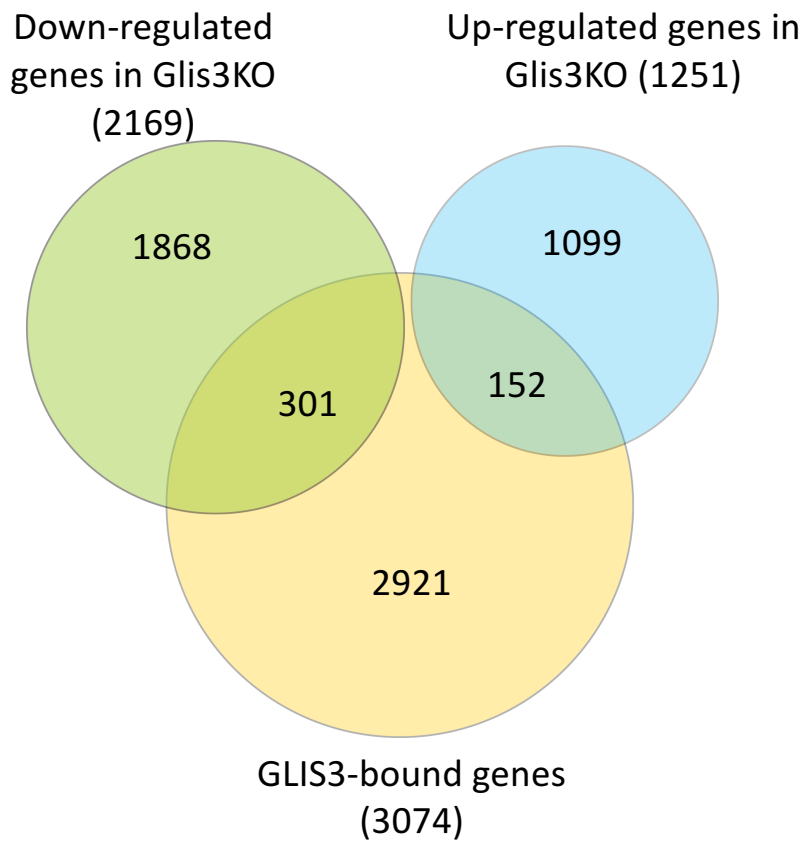

Supplemental Figure 9

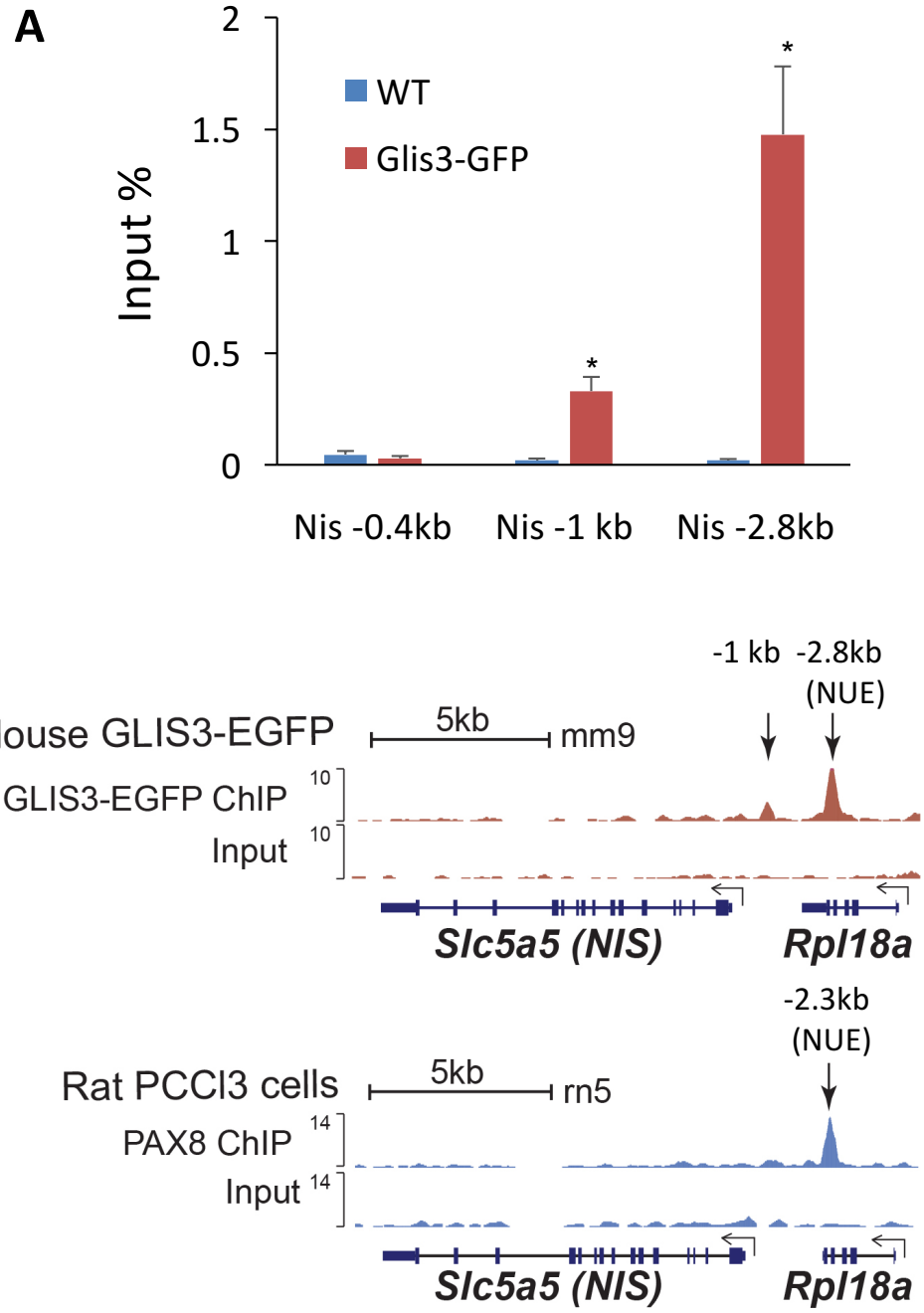

Supplemental Figure 10

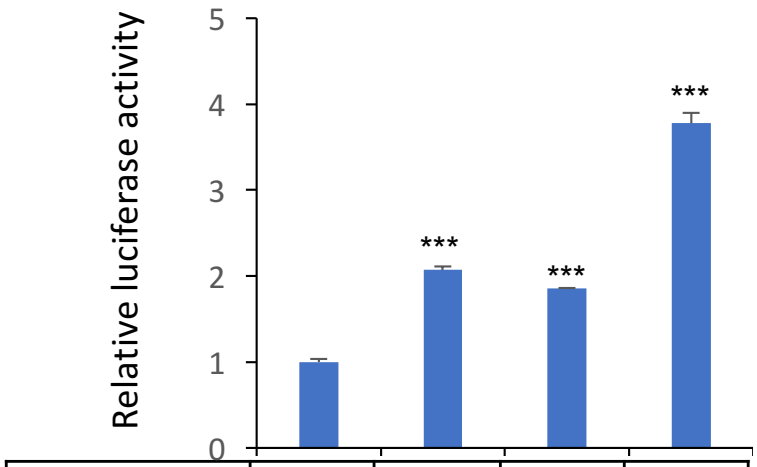

pTAL-NUE	+	+	+	+
Glis3	-	+	-	-
Pax8	-	-	+	+

Supplemental Figure 11

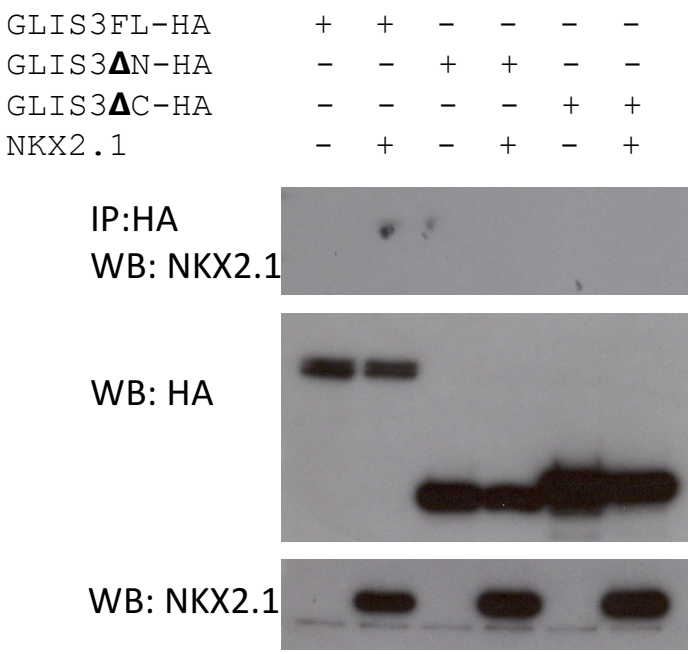

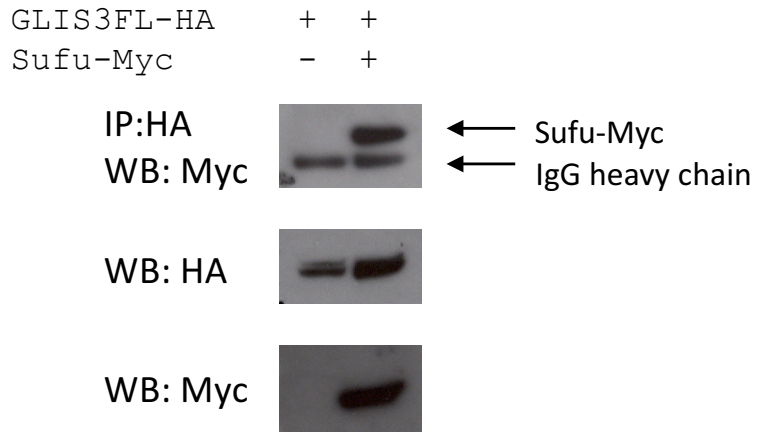

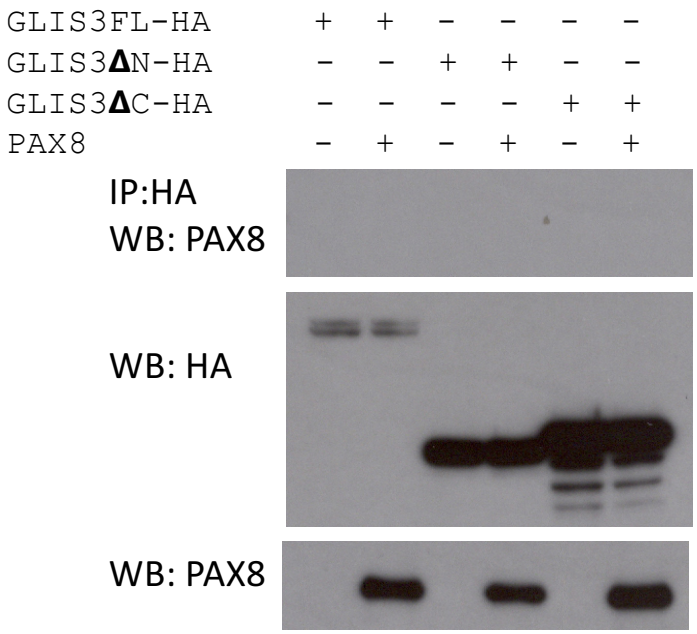

Supplemental Figure 12